FREE-SPACE COMMUNICATION LINK USING A GRATING LIGHT MODULATOR

D. Pedersen and O. Solgaard
Dept. of Electrical and Computer Engineering, 2064 Engineering II
University of California at Davis
Davis, CA 95616-5294

ABSTRACT

This paper presents the design and operation of a free-space communication link based on a Grating Light Modulator (GLM) in a corner-cube reflector configuration. A GLM is a micromachined optical phase grating whose grating efficiency can be controlled electrostatically. Combining the GLM with a corner cube to create a Grating Corner Cube (GCC) modulator reduces the alignment requirements of the device. Our device has a measured acceptance angle of $\approx 6^\circ$ in the plane of incidence of the GLM, limited by angle dependence of the grating. Significant improvement of the acceptance angle can be achieved by optimizing the layer thickness' of the grating structure. The resonance frequency of our GLM's are 290kHz. Their low damping leads to ringing that increases the switching time to 35us. Low misalignment sensitivity, low power consumption, and low switching times make the GCC ideal for use in free-space optical communication links.

INTRODUCTION

Micromachined corner cube reflectors have been previously demonstrated for use in free-space optical communication links [1][2]. These devices rely on the modulation of the orthogonality of the corner cube to encode signals on incident light as it is reflected back to its source. This orthogonality is modulated by electrostatic deflection of one of the mirror surfaces. However, the performance of these devices is limited by their slow mechanical response (1Kbps). In the Grating Corner Cube (GCC) modulator the retroreflection is modulated by a micrograting on one of the facets of the cube. The diffraction efficiency of the grating can be changed by application of an electric potential. When the grating is in the diffractive state, the light is not retroreflected. Changing the diffraction efficiency of the micrograting, therefore leads to modulation of the reflected light.

The active component of the GCC is the Grating Light Modulator (GLM) [3]. Arrays of these types of devices are being developed for display applications [4][5]. The GLM is composed of an array of periodically spaced ribbons suspended over an electrode. The ribbons effectively act as a reflection phase grating. When an electric potential is applied between the ribbons and the underlying substrate, they are electrostatically deflected downwards. This changes the path length difference for light reflected from the top of the ribbons and the underlying electrode. The net result is a change in the diffraction efficiency of the micrograting. The high stiffness and low mass of the GLM ribbons give them high resonant frequencies. GLM's have been switched at rates of <20ns [5]. Furthermore, the power consumption of the GLM is very low due to its small capacitance.

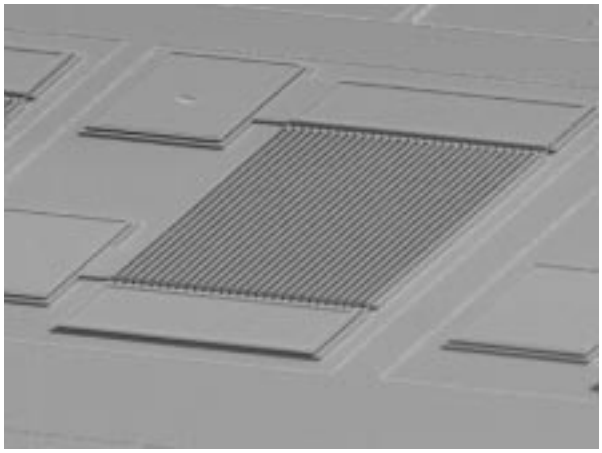

Figure 1: Scanning electron micrograph of a Grating Light Modulator. Ribbon array measures 150x200um

In this paper we discuss the design, construction, and testing of a grating corner cube modulator. We also present a coupled Boundary Element Method (BEM)/Finite Element Method (FEM) model of the grating light modulator and compare our simulation results to experimental data.

DESIGN AND FABRICATION

The basic GLM design uses a two layer surface micromachining process. The top layer is used to make the ribbon structures and the bottom layer is

used for the electrode. The ends of the ribbons are anchored to the substrate. We have fabricated these types of GLM devices using the MCNC Multi User MEMS Process (MUMPS). An scanning electron micrograph of a 150 by 200um GLM device is shown in figure 1. With the MCNC MUMPS process, we can fabricate the devices using either the polysilicon-1/polysilicon-2 (POLY1/POLY2) or polysilicon-0/polysilicon-1 (POLY0/POLY1) layers. This provides two different design choices for the electrode gap and ribbon thickness. The usage of the POLY1/POLY2 layers results in an electrode gap of 0.75um and ribbon thickness of 1.5um. In contrast, the POLY0/POLY1 layers result in an electrode gap of 2.0 um and a ribbon thickness of 2.0um. Fabrication using the POLY1/POLY2 layers results in devices with lower actuation voltages due to the reduced stiffness of the ribbons and the reduced size of the electrode gap. The reduced stiffness, however, lowers the resonant frequency of the device.

The GCC is comprised of three reflective surfaces, one of which is the GLM. The GCC is completed by transferring a set of orthogonal mirrors onto the chip containing the GLM. The passive mirrors are fabricated on pieces of cleaved silicon. A 4 inch, 500um thick silicon wafer is first sawed and cleaved into several pieces. Then 100nm of aluminum is evaporated onto the cleaved edge of the silicon. The two mirrors are assembled and transferred to the GLM chip.

NUMERIC SIMULATION

Our numeric simulation of the GLM consists of a finite element and boundary element model coupled together via the relaxation algorithm [6]. Figure 2 is an illustration of the BEM/FEM model used in our simulation. A two-dimensional boundary element model with constant flux and potential along the element is used to calculate the electric field in the region between the ribbon and electrode. The ribbon is simulated using a one-dimensional Euler-Bernoulli finite element beam model. The electrostatic boundary elements along the underside of the ribbon are coupled with the ribbon finite elements. The element nodes of the BEM model are used as the element nodes in the FEM model. Using the symmetry of the beam under deformation, only half of the region along the length of the ribbon is necessary for simulation. Fringing of the electrical field is corrected for with a precalculated correction factor. This factor is evaluated using the undeflected GLM to approximate fringing around the ribbon under small deflection.

Results of simulation of the center-point deflection of 3um wide, 200um long ribbons fabricated with POLY1/POLY2 layers are shown in figure 3. This coupled simulation uses 136 boundary elements and 64 finite elements. The figure shows a reasonable agreement between simulation and experimental results given the uncertainty in material constants and device geometry.

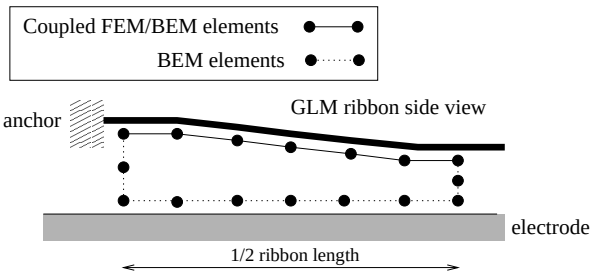

Figure 2: Boundary Element/ Finite Element model of Grating Light Modulator

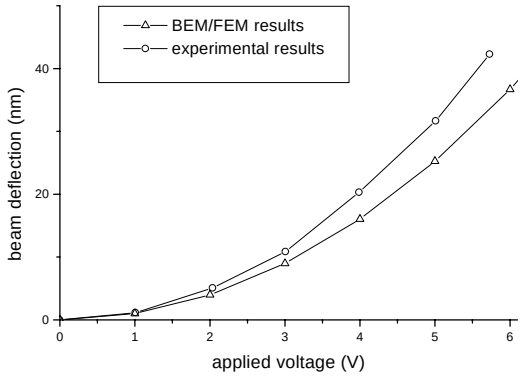

Figure 3: GLM numeric simulation results for center-point deflection

RESULTS

The basic GCC communication link is shown in figure 4. It consists of a GCC transmitter and a base station. The base station contains a laser source, quarter-wave plate, polarizing beam splitter, focusing lenses, and a photodetector. The base station uses a 635nm semiconductor laser with a collimating lens which yields a 720um collimated beam. A second lens is used to focus the beam down to a smaller spot. Focusing lenses with focal lengths of 25cm and 50cm have been used to provide variable working distances with the GCC, resulting in measured beam diameters of 44 um and 88 um at the waist, respectively.

A plot of the frequency response for a GLM with 200um long, 3 um wide, 1.5um thick ribbons is shown in figure 5. The ribbons have a resonance of 290kHz and are un-

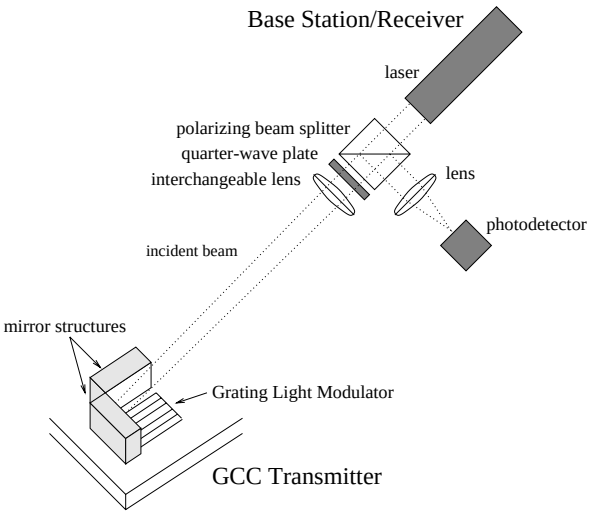

Figure 4: GCC free-space communication link

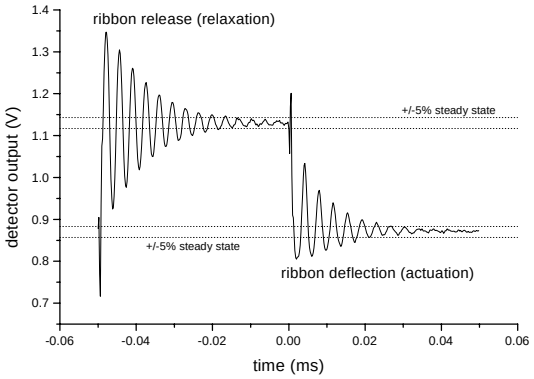

Figure 6: Step response of GCC modulator

der damped with a Q of 11.55 (damping coefficient of 0.045). The step response of the GCC is shown in figure

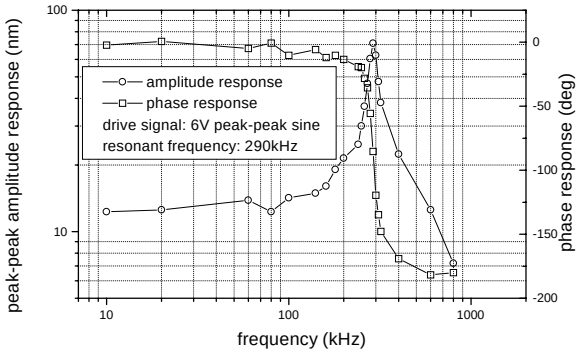

Figure 5: Frequency response for GLM with 3.0x1.5x200um ribbons

6. A 10V step input was used in generating this plot. The figure shows that the pull down transition and relaxation transition is damped differently. This can be explained by squeeze film damping [7][8] between the ribbons and the electrode. When the GLM's are actuated, the distance between the ribbons and the electrode is reduced. This increases the squeeze film damping for actuated transitions of the ribbons.

The observed resonant frequencies for the actuated and released transitions are 270kHz and 290kHz, respectively. There are two factors contributing to this frequency shift: the difference in squeeze film damping and the DC bias on the deflected ribbons. The increase in damping for the actuated GLM results in a relatively small shift of the natural damped response of the ribbons. The majority of the large observed frequency shift is due to the electrostatic deflection of the ribbons. The applied electrostatic field sets up a force that is increasing with decreasing ribbon electrode separation. This creates an "electrostatic spring" [9] that effectively reduces the ribbon spring constant and therefore the resonant frequency.

The ringing of the device is the limiting factor for the maximum data rate of the GCC. The settling time can be used as a conservative metric for determining the minimum amount of time after a state transition before the GLM can change states again. We define settling time as the time required for the step response of a system to settle within $\pm 5\%$ of steady-state. Settling time can be estimated using the following design formula for second order systems

$$t_s = \frac{3}{\xi \omega_n} \tag{1}$$

where ξ is the damping coefficient and ω_n is the natural frequency of the system. Using the results of the frequency response measurements, a settling time of 36.6us is calculated. This corresponds to a bit rate of 13.5kHz. The measured settling times from figure 6 are 24.8us for ribbon deflection and 35.0us for relaxation.

GCC's fabricated with the MUMPS process have a limited angle of operation due to the depth (or amplitude) of the grating structure. Deep grating structures result in a strong dependence of the effective grating depth on the incident angle of the light. GLM's fabricated with the POLY1/POLY2 layers have a grating depth of 2.25um

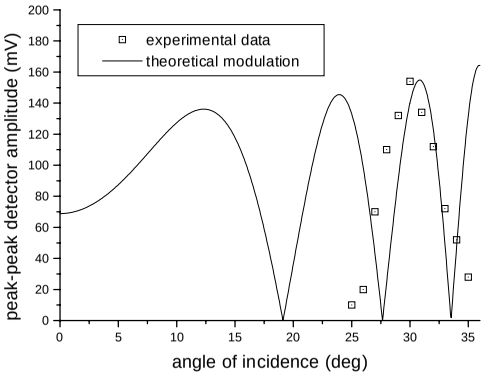

Figure 7: Angular acceptance of a GCC with a grating amplitude of 2.25um. The theoretical curve is found from eq. 2, combined with the responsivity of the detector. Experimental data were only obtained around an incident angle of $30°$.

or 3.54 wavelengths at 635nm.

The small signal modulation of the retroreflected light in a GCC is given by

$$\frac{dI}{ds} = \frac{2\pi I_0}{\lambda \cos\phi} \sin\left(\frac{4\pi s}{\lambda \cos\phi}\right) \qquad (2)$$

where ϕ is the angle of the incident light relative to the GLM facet, I_0 is the intensity of the incident light, s is the grating depth, and λ is the wavelength of the light. Figure 7 shows the theoretical small signal response for a POLY1/POLY2 GCC, together with the experimental results at the nominal incident angle of $30°$. The experimental results were obtained with 10V peak-peak sinusoidal actuation. The measured acceptance angle in the plane of incidence for FWHM is $\approx 6°$. The acceptance angle of the GCC in the plane orthogonal to the plane of incidence is limited only by the aperture of the corner cube reflector. Reducing the grating depth will sharply reduce the angle dependence of the GCC as can be seen from eq. 2.

CONCLUSION

We have demonstrated the Grating Corner Cube as a spatial light modulator for use in free-space communication links. These devices have been constructed in a two step process that starts with the fabrication of the GLM chip in a two-layer polysilicon surface micromachining process. The GCC is completed by the transfer of micro corner cube reflectors onto the chip

A numeric simulation of the GLM's has also been presented. The model is based on a coupled boundary element/finite element simulation of the GLM ribbons and shows good agreement with experimental results.

The GCC's noteworthy features include high-speed operation, low power consumption, and low alignment sensitivity. GCC switching times of ≈ 35us have been demonstrated and are limited by the ringing of the GLM ribbons. However, the 290kHz resonant frequency of the GLM ribbons suggests faster operation of the devices may be possible through prefiltering of the GLM control signal. This prefiltering can be used to condition the actuation voltage to minimize ringing of the device.

The measured acceptance angle of $6°$ significantly simplifies alignment of the GCC in a free-space optical communication link. The acceptance angle can be further improved through optimization of the fabrication process.

ACKNOWLEDGEMENTS

This work was funded by the California Industry and by the State of California UC-SMART program under contract 97-01.

REFERENCES

[1] D. Gunawan, L. Lin, and K. Pister. *Sensors and Actuators A*, 46-47:580–583, 1995.

[2] P. Chu, N. Lo, E. Berg, and K. Pister. *SPIE Proceedings*, 3008:190–201, 1997.

[3] Olav Solgaard. *Integrated Semiconductor Light Modulators for Fiber-Optics and Display Applications*. PhD thesis, Stanford University, 1992.

[4] D. T. Amm and R. W. Corrigan. *Society for Information Display Symposium*, 1998.

[5] R. B. Apte, F. S. A. Sandejas, W. C. Banyai, and D. M. Bloom. *Society for Information Display Symposium*, 1993.

[6] N.R. Aluru and J. White. *Proceedings IEEE Solid-State Sensors and Actuators Workshop*, pages 54–57, 1996.

[7] R. K. Gupta and S. D. Senturia. *Proceedings Tenth International Workshop on Micro Electro Mechanical Systems*, pages 290–294, 1997.

[8] Y. J. Yang, M. A. Gretillat, and S. D. Senturia. *Proceedings International Conference on Solid-State Sensors and Actuators*, pages 1093–1096, 1997.

[9] W. A. Clark, R. T. Howe, and R. Horowitz. *Technical Digest Solid-State Sensor and Actuator Workshop*, pages 283–287, 1996.